Nonlinear conductance fluctuations in quantum wires: Appearance of two different energy scales

A. Levy Yeyati
Departamento de Física de la Materia Condensada CXII, Universidad Autónoma de Madrid, E-28049 Madrid, Spain
(Received 16 May 1991)

Using a nonequilibrium Green-function formalism we study numerically the conductance fluctuations in a quantum wire as a function of the applied bias. This system is represented by a tight-binding Hamiltonian with random site energies and the current through the wire is expressed in terms of a transmission coefficient that can be computed by a recursive algorithm. We analyze the fluctuations in the transmission and in the differential conductance for different degrees of disorder, in the limit where the applied bias is much larger than the Thouless correlation energy E_c. In addition to the expected fluctuations in the E_c scale the conductance has also large random oscillations in a second energy scale related to the motion in the transverse direction. Electron heating effects are included in the model by means of an approximate self-energy, taking into account electron-electron interactions. An estimate is given of the typical voltage scales at which the effects described in this work might be observed in real metallic and semiconducting wires.

I. INTRODUCTION

The observation of universal conductance fluctuations in 1984 (Ref. 1) was followed by many theoretical[2–8] and experimental[9,10] works showing that this phenomena was a remarkable manifestation of quantum coherence.

The fluctuations can be observed in mesoscopic samples of size L much larger than the elastic mean free path and smaller than the phase coherence length L_Φ, as a function of an applied magnetic field or, in the case of semiconducting devices, by varying the Fermi energy. It was also shown that the shape of the fluctuation pattern is extremely sensitive to small changes in the impurity potential.[11]

The theoretical investigations of these effects include diagrammatic perturbation approximations,[2,3] the theory of random matrices,[4,5] and numerical simulations.[6–8]

On the other hand, the occurrence of random conductance fluctuations as a function of the applied bias, beyond the limit where linear response is expected to be valid, has been the object of only a few investigations. In 1986 Larkin and Khmel'nitskii,[12] using diagrammatic perturbation techniques, predicted that the current-voltage (I-V) characteristic of a mesoscopic sample should fluctuate around its Ohmic behavior with a typical voltage scale $V_c \sim E_c/e$, E_c being the Thouless correlation energy. Their work is based on the diffusion approximation, valid in the limit of weak disorder, and they obtain an integral expression for the conductance autocorrelation function. On the experimental side, Webb *et al.*[13] studied the conductance fluctuations as a function of the injected current in small metallic wires and rings, in a regime which corresponded to $V \gg V_c$. Although their results for the fluctuations amplitude are in qualitative agreement with the theory of Larkin and Khmel'nitskii, the behavior of the current correlation scale remains unexplained. In another experimental work, de Vegvar *et al.*[14] observed second-harmonic generation in quantum wires fabricated in GaAs-Al-Ga-As heterostructures, in the limit $eV \ll E_c$ where nonlinearities are small perturbations away from linear-response.

At this point, numerical work would be of interest in order to analyze in detail the nature of the conductance fluctuations when linear-response theory is no longer valid.

In this paper we present a numerical study of the nonlinear conductance of a disordered mesoscopic wire, represented by a two-dimensional tight-binding model with random site energies. Our results may illuminate different aspects of the problem that cannot be handled analytically. For example, we are not restricted to the limit of weak disorder but may consider the case of strong disorder as well. Also, the validity of the hypothesis of equivalence between energy and ensamble averages, used in most theoretical works, may be tested.

In order to obtain the total current through the system for a given applied bias we employ the Green-function formalism adapted by Keldysh[15] to deal with nonequilibrium situations. This technique was used by Caroli *et al.*[16] to obtain the tunneling current through insulating barriers and has been used recently by some authors[17,18] due to the feasibility of including many-body effects in a relatively simple way. The model and formalism used are described in the next section.

The third section is devoted to the numerical results and is divided into three parts. In the first we analyze the fluctuations in the transmission coefficient introduced in Sec. II. In the limit of linear response this is equal to the conductance, but the applied electric field produces some differences from the expected universal behavior. The second part describes the fluctuations in the nonlinear conductance as a function of the bias and the degree of disorder. The amplitude and the relevant energy scales in the conductance fluctuations are analyzed. Finally, in the third part we present an approximate description of the inelastic effects, with particular attention to the role

of electron heating induced by the applied bias.

In the last section we give the concluding remarks where we discuss some scaling arguments relating our numerical results to the nonlinear conductance fluctuations that might be observed in real semiconducting or metallic wires.

II. DESCRIPTION OF THE MODEL AND METHOD

The sample is represented by a rectangular strip defined on a square lattice. This strip is N sites long and M sites wide and we shall consider only the case $N \gg M$ for which a quasi-one-dimensional character is expected.

The system is described by a first-neighbors tight-binding Hamiltonian with a constant hopping parameter t taken as unit of energy. The disorder is introduced in the site energies that are randomly chosen in the range $-W/2$ to $W/2$ as in the usual Anderson model.

The ends of the sample are attached to semi-infinite and wider regions on which the site energies are constant. These represent the leads that fix the electrochemical potential difference on the sample. A given bias V is imposed by taking the site energies on the left lead as zero and equal to $-eV$ on the right lead. On the disordered central region the electrostatic potential is assumed to drop linearly from zero to $-eV$. This is taken into account by adding a term $-eVj/N$ to the site energies on the transversal row j.

In the Keldysh formalism, besides the usual retarded and advanced Green functions (G^r and G^a), two additional operators denoted by G^{+-} and G^{-+} are defined. These are related to the occupation probabilities in the nonequilibrium state. The total current through the system can be expressed in terms of the elements of G^{+-} as[16]

$$I = \frac{2et}{h}\int_{-\infty}^{\infty} \mathrm{Tr}\left[\mathbf{G}_{10}^{+-} - \mathbf{G}_{01}^{+-}\right] dE, \tag{1}$$

where Tr indicates trace operation over all sites in a row, and the notation $\mathbf{G}_{jk}$ denotes a $M \times M$ matrix whose elements $(\mathbf{G}_{jk})_{mm'}$ are $\langle jm \mid G \mid km' \rangle$.

At the steady state, the current must be equal on each row and thus, for convenience, we choose to calculate it at the interface between the left lead and the central region.

In order to obtain the relevant Green-function elements the coupling between rows 0 and 1 may be treated as a perturbation. The corresponding Dyson's equations are[16]

$$G^{+-} = \left[1 + G^r\Sigma^r\right] G^{(0)+-} \left[1 + \Sigma^a G^a\right] + G^r\Sigma^{+-}G^a,$$
$$G^{r,a} = G^{(0)r,a}\left[1 + \Sigma^{r,a}G^{r,a}\right]. \tag{2}$$

The appropiate self-energies in this case are

$$\mathbf{\Sigma}_{jk}^{r,a} = t(\delta_{0j}\delta_{1k} + \delta_{1j}\delta_{0k})$$

and $\mathbf{\Sigma}_{jk}^{+-} = 0$. As will be discussed later Σ^{+-} is different from zero only when many-body interactions giving rise to inelastic effects are considered.

The unperturbed functions $G^{(0)}$ correspond to two isolated regions which are in thermodynamic equilibrium (the chemical potential takes the value μ on the left lead and $\mu - eV$ on the rest of the system). Thus, these functions can be obtained using the usual techniques for systems in equilibrium.

As in a previous work[19] we calculate $G^{(0)r,a}$ using the recursive equations:

$$\mathbf{G}_{11}^{(0)}(z) = \mathbf{g}_1(z) = \left[z - \mathbf{H}_{11} - t^2\mathbf{g}_2\right]^{-1},$$
$$\mathbf{g}_j(z) = \left[z - \mathbf{H}_{jj} - t^2\mathbf{g}_{j+1}\right]^{-1}, \quad j \le j \le N \tag{3}$$

where $\mathbf{H}_{jj}$ is the projection of the Hamiltonian onto the subspace associated with row j. The input for these equations are the Green functions for the uncoupled leads, which are obtained from the conditions

$$\mathbf{g}_0(z) = \left[z - \mathbf{H}_{00} - t^2\mathbf{g}_0\right]^{-1},$$
$$\mathbf{g}_{N+1}(z) = \mathbf{g}_0(z + eV) \tag{4}$$

that can be easily solved if the eigenvalues and eigenvectors of $\mathbf{H}_{00}$ are known.

On the other hand, the elements of $G^{(0)+-}$ needed to solve (2) for $\mathbf{G}_{10}^{+-}$ and $\mathbf{G}_{01}^{+-}$ are given by

$$\mathbf{G}_{00}^{(0)+-} = f_L(\mathbf{g}_0^a - \mathbf{g}_0^r) \quad \text{and} \quad \mathbf{G}_{11}^{(0)+-} = f_R(\mathbf{g}_1^a - \mathbf{g}_1^r),$$

where f_L and f_R are the Fermi factors for the left- and right-hand sides of the uncoupled system.

Taking into account Eqs. (1), (2), and (3) we obtain the following expression for the total current at zero temperature:

$$I = \frac{2e}{h}\int_{\mu - eV}^{\mu} T(E,V)dE,$$
$$T(E,V) = 2t^2\mathrm{Tr}[\mathrm{Im}(\mathbf{g}_0^a)\mathbf{D}_{10}^r\mathrm{Im}(\mathbf{g}_1^a)\mathbf{D}_{01}^a], \tag{5}$$

where $\mathbf{D}_{jk} = (\mathbf{1} - t^2\mathbf{g}_j\mathbf{g}_k)^{-1}$. This expression is a generalization to the case of many quantum channels of the known result for the tunneling current in 1D systems.[16] A similar formula was derived by Martín-Rodero, Ferrer, and Flores[20] for a one-dimensional tight-binding system with many orbitals per site. Note that the function $T(E,V)$ can be considered as a transmission coefficient from left to right, and thus (5) is equivalent to the usual Landauer formula for nonlinear response.[21].

It is worth mentioning that an equivalent but more symmetrical expression, with respect to the left and right leads, can be obtained assuming that the perturbation involves the coupling between the central region and both leads. In this case the resulting expression is

$$T(E,V) = 2t^4\mathrm{Tr}[\mathrm{Im}(\mathbf{g}_0^a)\mathbf{G}_{1N}^r\mathrm{Im}(\mathbf{g}_{N+1}^a)\mathbf{G}_{N1}^a] \tag{6}$$

[see the Appendix for a direct proof of the equivalence

between (5) and (6)]. Also let us mention that the conductance can be calculated taking the derivative of (5) with respect to V, which gives

$$G(V) = \frac{2e^2}{h}\left[T(\mu - eV, V) + \int_{\mu - eV}^{\mu} \frac{\partial T}{\partial V} dE\right], \quad (7)$$

where the derivative $\frac{\partial T}{\partial V}$ can be expressed in terms of $\frac{\partial g_1}{\partial V}$ and $\frac{\partial g_0}{\partial V}$, which can be obtained using a recursive algorithm similar to that of Eqs. (3). In the limit of small applied bias we reobtain the well-known many-channel conductance formula $G = \frac{2e^2}{h}T$.

To keep a reasonable computational cost the main results presented in next section were obtained for the case $N = 10M$ with $M = 10$.

III. RESULTS

A. Fluctuations in the transmission coefficient

The transmission coefficient T displays random fluctuations as a function of the energy E and the applied bias V. An example of the typical patterns obtained for T is shown in Fig. 1. It can be observed that the fluctuations amplitude is of order 1, as expected from the theory of universal conductance fluctuations.[2] Also, in spite of their complex structure, it is possible to distinguish wide regions including several oscillations in a small energy scale, separated by large dips in the transmission.

According to the ergodic hypothesis used in most theoretical approaches,[2] averages of any function of T over the energy must be equal to an ensamble average over many different realizations of the disorder. We thus start our analysis by calculating the mean value $\langle T \rangle$ and the mean-square deviation of T defined as

$$T_{\rm rms} = \sqrt{\langle T^2 \rangle - \langle T \rangle^2},$$

where the angular brackets denote ensamble averaging. We consider about 200 random configurations in our averages and study the dependence of $\langle T \rangle$ and $T_{\rm rms}$ on the disorder strength W and the voltage V.

The results shown in Fig. 2 correspond to W in the range 0.20 to 2.0 and values of V up to 2 (measured in units of t/e). When W is small compared to V, both $\langle T \rangle$ and $T_{\rm rms}$ are sensitive to the applied field and decrease with increasing V. In this case the system is near the ballistic regime and the electric field introduces reflections in the band edges that reduce the transmission. On the other hand, when W is sufficiently large both $\langle T \rangle$ and $T_{\rm rms}$ become independent of V. The values of $T_{\rm rms}$ for $1 < W < 3$ are in good agreement with the value 0.36 predicted by the theory of universal conductance fluctuations for a one-dimensional geometry.[2]

Another way to analyze the same results is to plot $T_{\rm rms}$ against $\langle T \rangle$. This should reveal if there is a universal relation between both magnitudes, regardless of the degree of disorder or the energy, as expected from a single-parameter theory of localization. This plot is shown in Fig. 3, where three regions can be clearly identified. For large $\langle T \rangle$ ($\langle T \rangle > 3$) there is no universal relation between $T_{\rm rms}$ and $\langle T \rangle$ because the field acts to suppress the fluctuations and reduce $\langle T \rangle$ in this region. In contrast, for $1 \leq \langle T \rangle \leq 3$, $T_{\rm rms}$ is approximately constant and equal to the theoretically expected value. Thus, this region corresponds to what is called the diffusive regime.

Also for strong disorder ($\langle T \rangle \leq 1$) the relation between $T_{\rm rms}$ and $\langle T \rangle$ seems to be universal, but here $T_{\rm rms}$ tends to zero almost linearly with $\langle T \rangle$, as was found in previous numerical works.[7,8]

Another important feature in the fluctuations of T is the energy correlation scale E_c. In order to estimate E_c we have calculated the autocorrelation function $F(\Delta E)$, defined as

$$F(\Delta E) = \langle T(E)T(E + \Delta E) \rangle - \langle T \rangle^2$$

but here the brackets include an average over the energy for an energy range much larger than the expected E_c. The half width in the autocorrelation peak at $\Delta E = 0$ gives then a measure of E_c.

The results for $F(\Delta E)$ are shown in Fig. 4(a). As expected E_c decreases for increasing disorder, going from 0.042 for $W = 0.5$ to 0.008 for $W = 3$. Like $T_{\rm rms}$, E_c

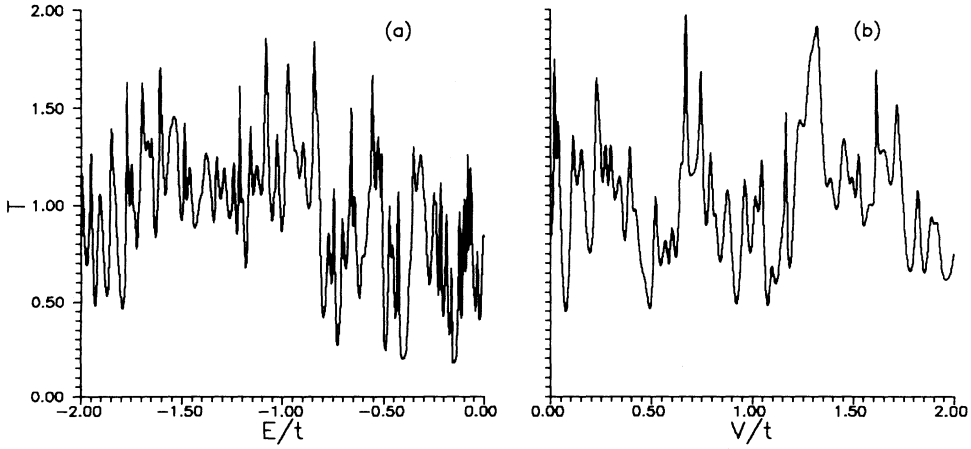

FIG. 1. Fluctuations in the transmission coefficient as a function of the energy (a) and of the applied voltage (b). These results correspond to a given disorder configuration with $W = 2$, the system size being $M = 10$ and $N = 100$.

was found to be rather insensitive to the applied field for $\langle T \rangle \leq 3$.

In this regime we also found a good agreement between the energy-averaged value $F(0)$ and the ensemble-averaged value $T^2_{\rm rms}$. However, the dependence of T on E is not completely random because, in that case, $F(\Delta E)$ should tend smoothly to zero for $\Delta E > E_c$. In contrast, as shown in Fig. 4(b), there are always some important correlations on an energy scale much larger than E_c and a second peak clearly appears in $F(\Delta E)$ for $\Delta E \gg E_c$, as indicated by an arrow in this figure. Let us call this second energy scale E_{c_2}. As will be shown in the next subsection this has an important effect on the conductance fluctuations when $V \gg E_c$.

In the same sense as E_c is related to the time of diffusion in the longitudinal direction, we may associate

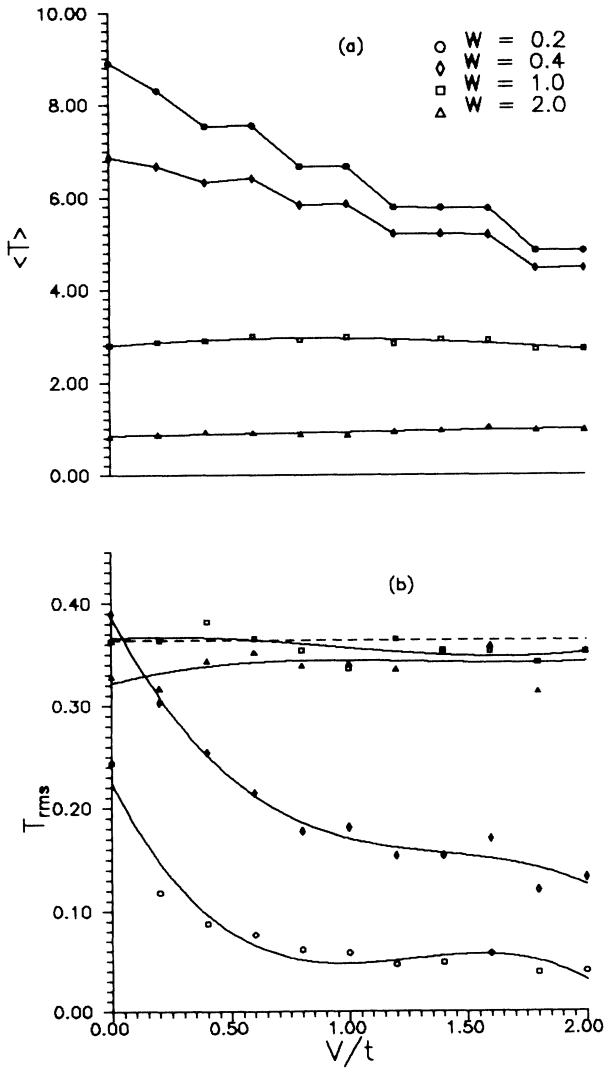

FIG. 2. (a) Mean value of the transmission coefficient $\langle T \rangle$ and (b) root-mean-square deviation $T_{\rm rms}$ against the applied bias for different values of W. These results were obtained averaging over 200 random configurations with $E = 0$. The dashed horizontal line indicates the universal value expected for a 1D geometry.

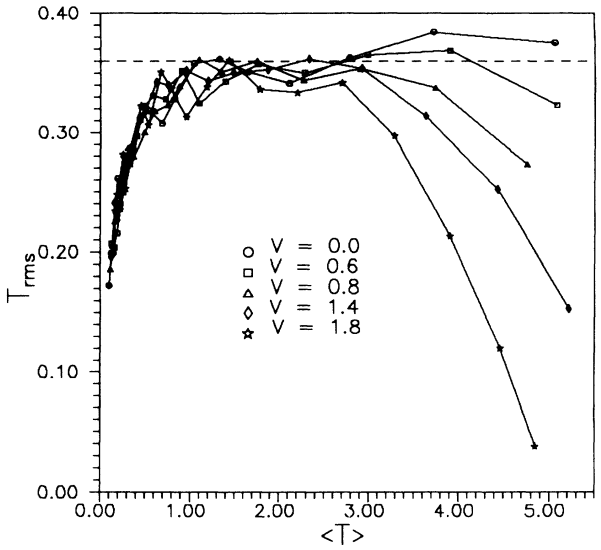

FIG. 3. $T_{\rm rms}$ against $\langle T \rangle$ for different values of the applied bias V. The dashed horizontal line has the same meaning as in Fig. 2(b).

E_{c_2} with the motion in the transverse direction. In a perfect sample this gives rise to the appearance of one-dimensional subbands with a typical spacing inversely proportional to the sample width. We confirmed that E_{c_2} is related to this effect by computing the autocorrelation function for different number of sites M, while keeping the ratio M/N constant. The larger energy scale E_{c_2} was found to behave roughly as M^{-1} while E_c/E_{c_2} remained almost constant.

B. Nonlinear conductance fluctuations

In order to obtain the differential conductance we carry out the numerical integration of Eq. (5) giving the total current, at two nearby bias conditions such as $\Delta V \ll E_c$. A good accuracy is obtained taking the integration step much smaller than E_c. Alternatively, the conductance may be obtained computing directly T and $\frac{\partial T}{\partial V}$ and using Eq. (7), but we found that both procedures give the same accuracy and are similarly time consuming.

In the region of small V ($V \ll E_c$), where linear response is expected to be valid, the conductance must behave as the transmission coefficient. The more interesting effects appear for large V, where the fluctuations of $G(V)$ are qualitatively different from those observed in T.

In Fig. 5 we show some examples of the typical traces obtained for G as a function of V for a particular disordered configuration and different values of W. In all cases the main features of these curves are random oscillations on a voltage scale corresponding to E_{c_2} and with an amplitude that increases for increasing V. From the curves in Fig. 5 and also from the autocorrelation of the transmission coefficient, E_{c_2} can be estimated to be 10 to 20 times larger than the corresponding E_c.

On the other hand, when the disorder is large enough ($\langle T \rangle \leq 1$) and when $V \gg E_c$ we find regions of

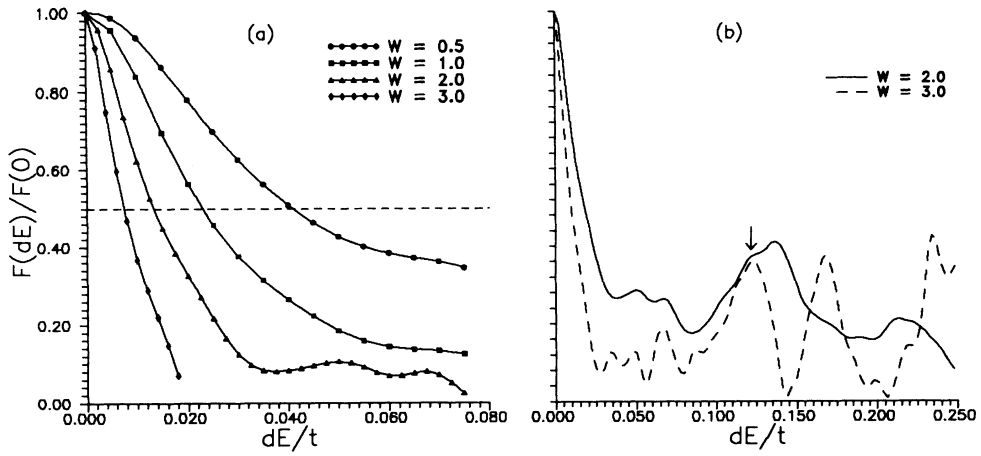

FIG. 4. (a) Autocorrelation function $F(\Delta E)$ for the transmission coefficient. The energy correlation scale is determined by the condition $F(E_c) = F(0)/2$. (b) $F(\Delta E)$ on a larger energy scale. The peak indicated by an arrow is used to define the second energy scale E_{c_2}.

negative conductance as was suggested by Larkin and Khmel'nitskii.[12]

If we analyze carefully one of these curves we find that the smaller fluctuation scale determined by E_c is clearly present at small V, but tends to disappear as V increases. This can be observed in Fig. 6 where the conductance for $W = 2$ is plotted with a larger resolution in the voltage scale. It can be said that the applied bias produces a self-averaging of the fluctuations on the smaller energy scale for $V \gg E_c$, while the fluctuations on E_{c_2} dominate until $V \gg E_{c_2}$. Unfortunately, due to computational limitations we are not able to analyze this limit (which would require $M \gg 10$ in order to keep V smaller than the total bandwidth). We expect however that a similar self-averaging effect takes place in this case.

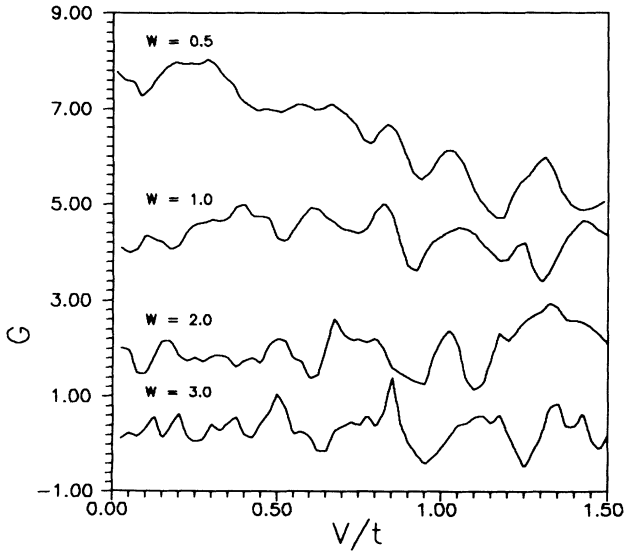

FIG. 5. Typical traces obtained for the differential conductance $G(V)$ (in units of $2e^2/h$) with increasing disorder. The distance between calculated points is $\Delta V = 0.05$.

C. Inelastic-scattering effects

In real samples the conductance will always be affected to some extent by inelastic scattering. Even when the temperature is low enough ($kT \ll E_c$), the applied bias induces an effective electron heating, thus degrading the phase coherence length.

This effect may be qualitatively described within our model by means of an approximate self-energy taking into account electron-electron or electron-phonon interactions. We shall concentrate here on the case of electron-electron interactions[22] represented by a Hubbard-type local repulsion term added to the one-electron Hamiltonian. To keep a simple picture it is necessary to assume that this self-energy is short ranged in space so that it can be well approximated by an on-site term. This should be a rather good approximation for a local electron-electron interaction.[24]

In this condition Caroli *et al.*[23] have shown that the total current may be split into two terms. First, an *elas-*

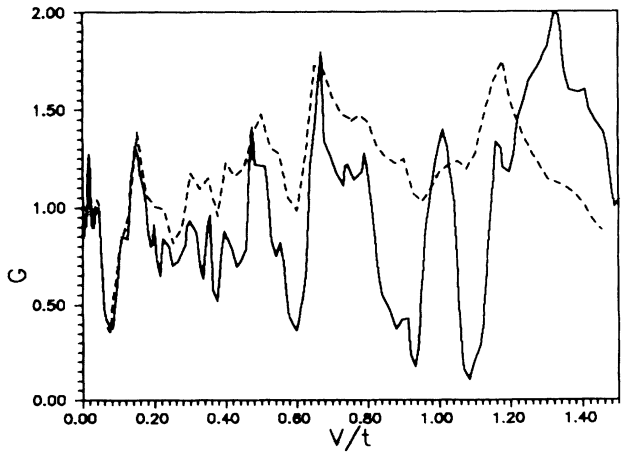

FIG. 6. Same curve as in Fig. 5 for $W = 2$ with a larger resolution in the V scale ($\Delta V = 0.005$).

tic contribution given by expression (5), but with the retarded and advanced propagators in T corrected by a term Σ^r_{ii} and Σ^a_{ii} respectively added to the site energies. This represents a mean-field potential giving a finite lifetime to the electronic states. Second, an *inelastic* contribution due to the Σ^{+-} term in Eq. (3) for G^{+-}, given by

$$I = \frac{2et^2}{h}\int_{-\infty}^{\infty}\sum_i \mathrm{Tr}\left[\mathbf{G}^r_{1i}\boldsymbol{\Sigma}^{+-}_{ii}\mathbf{G}^a_{i0} - \mathbf{G}^r_{0i}\boldsymbol{\Sigma}^{+-}_{ii}\mathbf{G}^a_{i1}\right] dE. \tag{8}$$

To proceed further we follow the prescriptions given in Ref. 17 and neglect the energy and site dependence of Σ^r, Σ^a, and Σ^{+-}. This should be valid for a small applied bias as compared to the total bandwidth. In this way, the inelastic effects are included in our model by means of a single parameter η, such that $\Sigma^r = \Sigma^a = i\eta$ and

$$I = \frac{2et^2}{h}\eta\int_{\mu-eV}^{\mu}\mathrm{Tr}\left[\sum_i(\mathbf{G}^r_{1i}\mathbf{G}^a_{i1})\mathrm{Img}^a_0\right] dE. \tag{9}$$

Note that η is nothing but an average of the self-energies over the energy range between $\mu - eV$ and μ.

We are interested in the dependence of this parameter with the applied bias. This can be estimated by an approximate calculation to second order in the electron-electron interaction.[25] Assuming a rectangular density of states this calculation yields[17]

$$\eta \simeq \frac{U^2V^2}{W_b^3},$$

where U is the on-site electronic repulsion and W_b is the total bandwidth. For a metallic system U/W_b may be assumed to be of order 0.1. Thus, as V increases the inelastic contribution to the total energy increases and, for strong disorder, it may be even larger than the elastic contribution. At the same time, the fluctuations of the transmission coefficient and, consequently, of the conductance, will be damped due to the energy-level broadening introduced by η.

In Fig. 7(a) we show the rms value of T as a function of V when inelastic effects are included. It can be observed that T_{rms} remains almost constant when V is such that $\eta \ll E_c$ and decays roughly as V^{-1} for larger values of V.

The incidence of inelastic effects on the conductance is rather similar. The dashed line in Fig. 6 represents the conductance as a function of V when inelastic effects are included. We observe that, except for the small-V region, the oscillations are substantially reduced. The rms value of G however has a smoother decay with V than T_{rms} has, as can be seen in Fig. 7(b). The arrows in this figure indicate the values of V for which $\eta \simeq E_c$ and $\eta \simeq E_{c_2}$, respectively. Only when $\eta \simeq E_{c_2}$ we find that G_{rms} is of the same order as T_{rms}.

IV. CONCLUDING REMARKS

The main physical result of this work is the identification of a second energy scale E_{c_2} larger than E_c, that plays an important role on the conductance fluctuations when $V \gg E_c$.

In order to relate our model calculations to real experimental situations, an estimate of E_{c_2} and E_{c_2}/E_c in real devices must be given. An upper bound to E_{c_2} is certainly given by the typical subband spacing in a perfect wire. For a metallic wire like those used in Ref. 13, assuming that the number of occupied channels is approximately given by $N_{\mathrm{ch}} \simeq (L_t/\lambda_F)^2$ (where L_t, the transverse length, is of order of 300 Å, while λ_F, the Fermi wavelength, is about 1 Å), we obtain $E_{c_2} \simeq 20$ μeV. This has to be compared with the estimation of E_c given in the same reference, that is 1–2 μeV. On the other hand, the typical subband spacing for quantum wires fabricated on Si MOSFET devices have been measured giving 2–4 meV,[26] while typical values of E_c in these systems are 0.1 meV.[9]

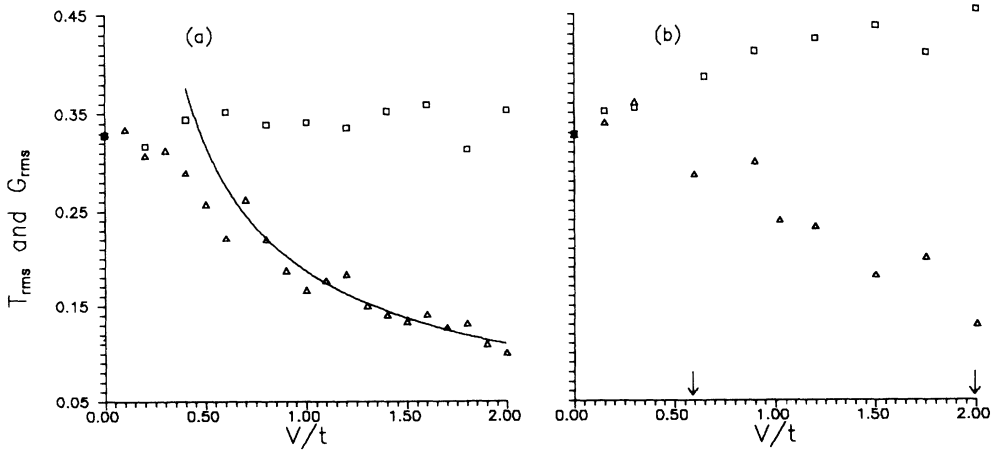

FIG. 7. T_{rms} (a) and G_{rms} (b) for $W = 2$ with (triangles) and without (squares) inelastic effects as explained in text. The solid curve in (a) is a numerical fit that yields $T_{\mathrm{rms}} \sim V^{-0.9\pm0.1}$. The arrows in (b) indicate the values of V for which $\eta \simeq E_c$ and E_{c_2}, respectively.

Thus, both estimations lead us to the conclusion that E_{c_2}/E_c is between 10 and 20 in metallic and semiconducting wires, in agreement with our numerical results. The nonlinear regime that we have studied in this work might correspond to a bias voltage larger than 20 μeV in metallic wires as those used in Ref. 13, and larger than 5 meV for semiconducting wires as those of Ref. 22. In fact, the experimental data presented in Fig. (a) of Ref. 13 strongly suggests the appearance of the second energy scale.

We must indicate that the occurrence of fluctuations in two energy scales has recently been reported in a different context, corresponding to large silicon inversion layers in the variable-range hopping regime.[27]

We have also shown how to include electron heating effects in our model, the main conclusion being that these do not suppress the conductance fluctuations in both energy scales unless V is much larger than E_c and E_{c_2}, respectively. This is due to the small factor U/W_b that relates V with the imaginary part of the self-energies.

Further experimental work would be of interest, especially on Si MOSFET quantum wires, in order to confirm the qualitative results presented here.

ACKNOWLEDGMENTS

The author wishes to thank S. Washburn for having called his attention to this problem and also J.V. José, F. Flores, and M. Weissmann for useful discussions. This work was supported by the Ministerio de Educación y Ciencia de España.

APPENDIX

In this appendix we demonstrate the equivalence between Eqs. (5) and (6). This equivalence is warranted by the fact that both expressions are exact to order infinity in the coupling parameter t. However this is masked by their different mathematical form and thus a direct proof of the equivalence should be desirable.

To proceed with the proof we first show that (6) may be written as

$$T(E,V) = 2t^4 \mathrm{Tr}\left[\mathrm{Im}(\mathbf{g}_0^a)\mathbf{G}_{1N'}^r \mathrm{Im}(\mathbf{g}_{N'+1}^a)\mathbf{G}_{N'1}^a\right], \quad 2 \le N' < N \tag{A1}$$

Let us consider the case $N' = N - 1$. From (3) it is easy to show that

$$2it^2 \mathrm{Im} g_{j+1}^a = \left[g_j^r\right]^{-1} - \left[g_j^a\right]^{-1}, \quad 1 \le j \le N. \tag{A2}$$

We also make use of the following relations:

$$\mathbf{G}_{1N}^r = t\mathbf{G}_{1N-1}^r \mathbf{g}_N^r, \qquad \mathbf{G}_{N1}^a = t\mathbf{g}_N^a \mathbf{G}_{N-11}^a. \tag{A3}$$

Replacing (A2) and (A3) in (6) we obtain (A1) for $N' = N - 1$. The same procedure may be applied recursively to go from (A1) with $N' = N - 1$ to the same expression with $N' = 2$. Using (A2) this may be written as

$$T(E,V) = i\mathrm{Tr}\left[\mathrm{Im}(\mathbf{g}_0^a)\mathbf{G}_{11}^r \left\{\left[g_1^a\right]^{-1} - \left[g_1^r\right]^{-1}\right\} \mathbf{G}_{11}^a\right]. \tag{A4}$$

Now the equivalence between (5) and (A4) [and therefore between (5) and (6)] is straightfoward if we first notice that

$$\mathbf{G}_{11}^r = \mathbf{D}_{10}^r \mathbf{g}_1^r, \qquad \mathbf{G}_{11}^a = \mathbf{g}_1^a \mathbf{D}_{01}^a. \tag{A5}$$

[1] C.P. Umbach, S. Washburn, R.B. Laibowitz, and R.A. Webb, Phys. Rev. B **30**, 4084 (1984).
[2] P.A. Lee and A.D. Stone, Phys. Rev. Lett. **55**, 1622 (1985).
[3] B.L. Al'tshuler, Pis'ma Zh. Eksp. Teor. Fiz. **41**, 530 (1985) [JETP Lett. **41**, 648 (1985)].
[4] Y. Imry, Europhys. Lett. **1**, 249 (1986).
[5] J.L. Phichard, in *Quantum Coherence in Mesoscopic Systems*, edited by B. Kramer (Plenum, New York, 1991).
[6] A.D. Stone, Phys. Rev. Lett. **54**, 2692 (1985).
[7] N. Giordano, Phys. Rev. B **36**, 4190 (1987); **38**, 4746 (1988).
[8] R. Harris and A. Houri, Phys. Rev. B **42**, 7266 (1990).
[9] J.C. Licini, D.J. Bishop, M.A. Kastner, and J. Melngailis, Phys. Rev. Lett. **55**, 2987 (1985).
[10] C.P. Umbach, C. VanHaesendonck, R.B. Laibowitz, S. Washburn, and R.A. Webb, Phys. Rev. Lett. **56**, 386 (1986).
[11] B.L. Alt'shuler and B.Z. Spivak, Pis'ma Zh. Eksp. Teor. Fiz. **42**, 363 (1985) [JETP Lett. **42**, 447 (1985)]; S. Feng, P.A. Lee, and A.D. Stone, Phys. Rev. Lett. **56**, 1960 (1986).
[12] A.I. Larkin and D.E. Khmel'nitskii, Zh. Eksp. Teor. Fiz. **91**, 1815 (1986) [Sov. Phys.— JETP **64**, 1075 (1986)].
[13] R.A. Webb, S. Washburn, and C.P. Umbach, Phys. Rev. B **37**, 8455 (1988). See also S. Washburn, in *Quantum Coherence in Mesoscopic Systems* (Ref. 5).
[14] P.G.N. deVegvar, G. Timp, P.M. Mankiewich, J.E. Cunningham, R. Behringer, and R.E. Howard, Phys. Rev. B **38**, 4326 (1988).
[15] L.V. Keldysh, Zh. Eksp. Teor. Fiz. **47**, 1515 (1964) [Sov. Phys.— JETP **20**, 10108 (1965)].
[16] C. Caroli, R. Combescot, P. Nozieres, and D. Saint-James, J. Phys. C **4**, 916 (1971).
[17] F. Flores and E.V. Anda (unpublished); E.V. Anda and F. Flores, J. Phys. Condens. Matter **3**, 9087 (1991).
[18] S. Datta, Phys. Rev. B **37**, 8455 (1988).
[19] A. Levy Yeyati, J. Phys. Condens. Matter **2**, 6533 (1990).
[20] A. Martín-Rodero, J. Ferrer, and F. Flores, J. Microsc. **152**, 317 (1988).
[21] R. Landauer, in *Localization, Interaction and Transport Phenomena in Impure Metals*, edited by G. Bergman, Y. Bruynsraede, and B. Kramer, Springer Series in Solid State Physics Vol. 61 (Springer, Berlin, 1985), p. 162.

[22] J.R. Gao, J. Caro, A.H. Vergruggen, S. Radelaar, and J. Middelhock, Phys. Rev. B **40**, 11 676 (1989). The experimental data presented in this work indicate that electron-electron interaction is the dominant inelastic-scattering mechanism in semiconducting samples at low temperatures.
[23] C. Caroli, R. Combescot, P. Nozieres, and D. Saint-James, J. Phys. C **5**, 21 (1972).
[24] A. Martín-Rodero, E. Louis, F. Flores, and C. Tejedor, Phys. Rev. B **29**, 476 (1984).
[25] First-order contributions to the self-energy yield only a rigid shift of the energy levels. In contrast, in second order the self-energies have an imaginary part leading to an energy-level broadening as dicussed in Ref. 24.
[26] J.R. Gao, C. de Graaf, J. Caro, S. Radelaar, M. Offenberg, V. Lauer, J. Singleton, T.J. Janssen, and J.A. Perenboom, Phys. Rev. B **41**, 12 315 (1990).
[27] D. Popovic, A.B. Fowler, S. Washburn, and P.J. Stiles, Phys. Rev. B **42**, 1759 (1990).